High-Volume Recycled Waste Glass Powder Cement-Based Materials: Role of Glass Powder Granularity

Akli Younsi, Mohammed Amar Mahi, Ameur El Amine Hamami, Rafik Belarbi, Emilio Bastidas-Arteaga

buildings

MDPI

Article

High-Volume Recycled Waste Glass Powder Cement-Based Materials: Role of Glass Powder Granularity

Akli Younsi [1,*], Mohammed Amar Mahi [1], Ameur El Amine Hamami [1], Rafik Belarbi [1,2] and Emilio Bastidas-Arteaga [1,*]

[1] LaSIE UMR CNRS 7356, La Rochelle University, Avenue M. Crépeau, 17042 La Rochelle Cedex 1, France; mahi.amarmohammed@gmail.com (M.A.M.); ahamami@univ-lr.fr (A.E.A.H.); rafik.belarbi@univ-lr.fr (R.B.)
[2] Department of Architecture, Canadian University Dubai, City Walk, Dubai P.O. Box 415053, United Arab Emirates
* Correspondence: akli.younsi@univ-lr.fr (A.Y.); ebastida@univ-lr.fr (E.B.-A.)

Abstract: The use of recycled waste glass powder (RWGP) as a partial substitute for cement in cement-based materials offers a promising solution for reducing environmental impact and promoting sustainable waste management practices. An experimental study was conducted on a reference material made with Portland-limestone cement CEMII/A-LL42.5R and three other materials containing 50 wt% RWGP with different mean diameters, d_{50}: 16, 18, and 25 µm. The main objective was to analyze the role of RWGP granularity in the short- and medium-term properties of the cement-based materials. The results showed that coarser RWGP granularity led to an increase in fluidity and Portlandite content, while water demand and mechanical properties decreased. However, the range of RWGP granularities tested did not significantly affect the initial setting time, fresh and dry density, hydration temperature, and water porosity. These findings suggest that the choice of RWGP granularity should depend on the desired properties of the cement-based material.

Keywords: recycled waste glass powder; cement-based materials; glass powder granularity; short-/medium-term properties

check for updates

Citation: Younsi, A.; Mahi, M.A.; Hamami, A.E.A.; Belarbi, R.; Bastidas-Arteaga, E. High-Volume Recycled Waste Glass Powder Cement-Based Materials: Role of Glass Powder Granularity. *Buildings* **2023**, *13*, 1783. https://doi.org/10.3390/buildings13071783

Academic Editor: Blessen Skariah Thomas

Received: 26 June 2023
Revised: 10 July 2023
Accepted: 11 July 2023
Published: 13 July 2023

1. Introduction

Cement production is not only energy- and resource-intensive, but also contributes significantly to global greenhouse gas (GHG) emissions, particularly with the release of carbon dioxide (CO_2) [1–3]. On average, the production of one ton of cement releases around 500 to 700 kg of CO_2 [1,2], making the cement industry responsible for approximately 7.4% of global CO_2 emissions [3]. Moreover, cement manufacturing accounts for about 70% of GHGs from the production of cement-based materials [4].

One commonly used approach to reduce CO_2 emissions from the production of cement-based materials is to partially substitute cement with supplementary cementitious materials (SCMs) [1,4], such as fly ash, ground granulated blast-furnace slag, natural pozzolans, silica fume, or limestone filler. Recently, researchers have been exploring the feasibility of using new SCMs, including recycled waste glass powder (RWGP) [5–7].

Designing new cement-based materials with RWGP as a partial substitute for cement offers several benefits. Firstly, it reduces the environmental impact of these materials by decreasing the amount of cement used [8]. By partially substituting cement with RWGP, the amount of cement used in cement-based materials is decreased, leading to a reduction in the systematic use of natural resources in cement composition. Furthermore, the use of RWGP as an SCM also avoids the need for some natural SCMs, such as limestone filler, further contributing to the reduction in natural resource usage in the production of cement-based materials [9]. Additionally, reusing waste glass as RWGP in cement-based materials helps to limit its landfill and contributes to a more sustainable waste management system.

Overall, this approach offers a promising solution for reducing the environmental impact of cement-based materials while promoting sustainable waste management practices [5–7].

Reusing waste glass to manufacture new recycled glass products can be performed multiple times without significantly altering its properties [10–12]. However, the process is often limited in many countries due to the variability in chemical properties of waste glass [12], caused by the mixing of waste glass of different colors [10–12] and small debris that is expensive to sort [10]. This hard-to-recycle waste glass is often landfilled, taking up valuable land resources [13] and potentially causing severe environmental issues due to its non-biodegradability [10,14]. Currently, the recycling rate of waste glass varies globally from approximately 13% in China [13] to around 70% in France [15]. The use of hard-to-recycle waste glass as RWGP to partially substitute cement in cement-based materials [5–7] can be an effective solution to increase the recycling rate of waste glass. It is worth noting that RWGP can also be employed as a substitute for cement in cemented tailing backfill applications [16,17].

When considering a fixed cement substitution ratio and a fixed water-to-binder ratio, the short- and long-term properties of cement-based materials designed with partial substitution of cement with RWGP are influenced by various factors, as outlined below:

Increase or decrease in slump/water demand—The increase in slump (corresponding to the decrease in water demand) when using RWGP is attributed to: (i) the smooth (glassy) [13] and hydrophobic [18] surface of the glass particles, and (ii) the coarser granularity of RWGP compared to cement [19]. This results in less friction between the particles and allows them to move more freely within the mixture [20]. On the other hand, the decrease in slump (corresponding to the increase in water demand) is attributed to: (i) the angular [15] and irregular [14] shape of the RWGP particles, which have a high aspect ratio [18] and sharp edges [21], and (ii) the finer granularity of RWGP compared to cement [13], despite the hydrophobicity of RWGP [11]. This results in more friction between the particles and a reduction in the flowability of the mixture [13].

Increase in initial setting time—The increase in initial setting time when using RWGP results from two factors. Firstly, there is a reduction in the overall hydration level resulting from both the cement dilution effect [22] (the cement dilution effect decreases the amount of clinker) and the slow pozzolanic reaction of RWGP at early age [23]. This delay in pozzolanic reaction occurs until there is an adequate amount of Portlandite present in the pore solution [12]. Secondly, there is a rise in the effective water-to-cement ratio due to both the cement dilution effect [14] and the hydrophobic nature of RWGP [19], which increases the amount of water actually available [12].

Decrease in fresh and dry density—The reduction in both fresh and dry density when using RWGP is due to the lower density of RWGP compared to cement [19,24].

Decrease in heat of hydration—The decrease in the amount of heat of hydration released when using RWGP comes from the reduction in the overall hydration level resulting from both the cement dilution effect [22] and the slow pozzolanic reaction of RWGP at early age [12].

Decrease in Portlandite content—The decrease in Portlandite content when using RWGP is attributed to two factors. Firstly, the reduction in the hydration level due to the cement dilution effect [25] leads to a decrease in Portlandite content. Secondly, the pozzolanic reaction of RWGP converts a portion of Portlandite into C-S-H [14]. Therefore, the reduction in Portlandite content can serve as an indicator of the pozzolanic activity of RWGP.

Increase in water porosity—The increase in water porosity when using RWGP is related to two factors. Firstly, there is a reduction in the overall hydration level resulting from both the cement dilution effect [23] and the weaker pozzolanic reaction of RWGP compared to the hydration of cement [18]. Secondly, there is a rise in the effective water-to-cement ratio due to both the cement dilution effect [21] and the hydrophobic nature of RWGP [26], which increases the amount of available water [12].

Decrease in mechanical properties—The decrease in mechanical properties when using RWGP, especially at early age, comes from two factors. Firstly, there is a reduction in the overall hydration level resulting from both the cement dilution effect [27], the weaker pozzolanic reaction of RWGP compared to the hydration of cement [18], and the slower pozzolanic reaction of RWGP at early age [23]. Secondly, there is a rise in the effective water-to-cement ratio due to both the cement dilution effect [21] and the hydrophobic nature of RWGP [13], which increases the amount of available water [12]. These factors contribute to the decrease in mechanical properties, particularly during early age.

Regarding the effect of RWGP granularity, it has been observed that for substitution ratios $\leq$ 40 wt%, the use of finer RWGP granularity leads to: (i) a decrease in fluidity [28] and Portlandite content [10], and (ii) an increase in the amount of heat of hydration released [29] and mechanical properties [30]. The behavior of Portlandite content, heat of hydration, and mechanical properties when using a finer RWGP granularity is attributed to a higher level of overall hydration, resulting from two factors: (i) the greater number of nucleation sites provided by RWGP [29], and (ii) the faster pozzolanic reaction of RWGP [10].

Despite numerous studies on cement-based materials containing RWGP, according to the authors' knowledge, there is still a lack research studies and standard recommendations on the following aspects: (i) the properties of materials with high cement substitution ratio, i.e., those that contain $\geq$50 wt% of RWGP (lack or absence of data) [21,23,31], (ii) the influence of RWGP granularity on material properties (lack or absence of data) [10,13,27], and (iii) the influence of RWGP granularity on properties of materials with high cement substitution ratio (absence of data).

Therefore, this study focuses on three previously mentioned aspects, with a specific emphasis on analyzing the role of RWGP granularity in the short- and medium-term properties of materials with cement substitution ratio of 50 wt%. This study will provide insights about the suitable RWGP granularity that should be envisaged to achieve given expected material properties (performance-based approach in future standards).

In this study, a reference mortar or paste was designed using Portland-limestone cement CEMII/A-LL42.5R without any RWGP, while three other mortars or pastes were designed using 50 wt% substitution of CEMII/A-LL42.5R with RWGP of three different mean diameters, d_{50}: 16, 18, and 25 µm. The three variants of RWGP were obtained from cleaning, crushing, and sieving of hard-to-recycle waste glass of different colors. The density, Blaine specific surface area, and particle size distribution of both cement and the different variants of RWGP were measured. The workability of freshly mixed mortars was characterized using a mini-conical slump test. Water demand and initial setting time were assessed on paste mixtures with normal consistency. Fresh density was obtained from freshly mixed mortars, while dry density was determined on 91-day mortar samples. The time-evolution of hydration temperature was studied by conducting semi-adiabatic calorimetry on freshly mixed mortars. The time-evolution of Portlandite content was obtained by thermogravimetric analysis on mortar powders at 1, 7, 28, and 91 days. The time-evolution of porosity was determined by water saturation under vacuum on mortar samples at 1, 7, 28, and 91 days. Finally, the time-evolution of flexural and compressive strength was monitored on mortar specimens at 1, 7, 28, and 91 days.

2. Materials and Methods

2.1. Source Materials

This study investigated four cement-based materials that were designed using Portland-limestone cement CEMII/A-LL42.5R (referred to as "CEMII" hereafter), which meets the EN 197-1 standard [32]. CEMII consists of 91% clinker and 9% limestone, and its chemical composition, as provided by the manufacturer (EQIOM France), is shown in Table 1. The density, Blaine specific surface area, and mean diameter d_{50} of CEMII are presented in Table 2. The density was measured using a Micromeritics AccuPyc II 1340® helium pycnometer in accordance with the ISO 12154 standard [33]. The Blaine specific surface area was determined using a Controls® Blaine fineness apparatus following the EN 196-6

standard [34]. The mean diameter d_{50} was obtained from the particle size distribution, as shown in Figure 1, which was acquired via a dry process using a CILAS 1090® laser diffraction particle size analyzer in compliance with the ISO 13320 standard [35].

Table 1. Chemical composition and loss of ignition (LOI) of CEMII [wt%].

CaO	SiO_2	Al_2O_3	Fe_2O_3	SO_3	MgO	K_2O	Na_2O	LOI
63.2	18.6	4.4	3.3	2.6	1.6	0.8	0.3	4.9

Table 2. Some physical properties of CEMII and different variants of RWGP.

	CEMII	RWGP16	RWGP18	RWGP25
Density [g/cm^3]	3.08	2.46	2.46	2.46
Blaine surface area [cm^2/g]	4236	3906	3327	2585
Mean diameter d_{50} [µm]	10.19	15.91	18.34	25.41

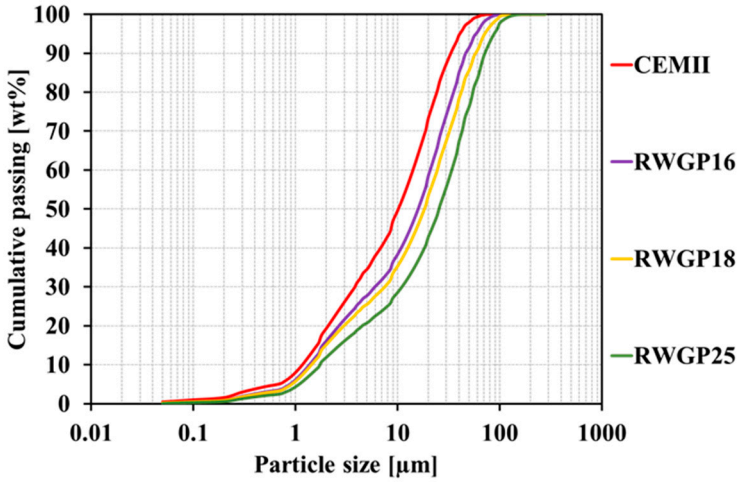

Figure 1. Particle size distributions of CEMII and different variants of RWGP determined by a laser diffraction particle size analyzer.

Three out of the four cement-based materials were formulated by substituting 50 wt% of CEMII with a recycled waste glass powder (RWGP), which was derived from hard-to-recycle waste glass of various colors obtained from the La Rochelle Waste Sorting Center in France. To obtain RWGP, the waste glass was immersed in tap water (renewed twice a day) for 16 days, followed by manual sorting to remove impurities. After air-drying for three days, the glass was crushed using a Retsch BB200® jaw crusher until it reached a particle size of less than 2 mm. This powder was then sieved to obtain three powders with different mean diameters, d_{50}: 16, 18, and 25 µm (Table 2). The d_{50} of 16 µm was achieved by using a sieve with a pass-through of 63 µm (granular class < 63 µm). Similarly, the d_{50} of 18 µm was obtained using a sieve with a pass-through of 80 µm (granular class < 80 µm). However, for the d_{50} of 25 µm, the powder was retained between sieves with openings of 63 and 80 µm (granular class between 63 and 80 µm). It is important to note that, despite all precautions taken, coarser particles than the sieves used are found in the final powder for each of the three granular classes studied. Additionally, in the granular class between 63 and 80 µm, it is worth noting that particles finer than 63 µm are still present in the final powder. This discrepancy explains the d_{50} of 25 µm, which falls outside the expected range of 63–80 µm. These findings are consistent with existing literature [10,36]. The powders were labeled as "RWGP16", "RWGP18", and "RWGP25", respectively, based on their mean diameters d_{50}. The densities, Blaine specific surface areas, and mean diameters d_{50} of each variant are listed in Table 2, and their particle size distributions, are depicted in Figure 1.

The data revealed that CEMII is finer than all three RWGP variants, with RWGP16 being the finest and RWGP25 being the coarsest based on their mean diameters d_{50}.

The mortar mixtures were formulated using siliceous sand with a particle size of 0/4 mm, which adheres to the EN 13139 standard [37]. This sand has a density of 2.49 g/cm^3 and a water absorption coefficient of 0.6%.

2.2. Mixture Proportions and Sample Preparations

Table 3 outlines the proportions utilized in the mortar mixtures that were examined. These mixtures were created using the mix-design method described by Equations (1)–(4):

$$V_C + V_G + V_W + V_S = 1\ m^3 \quad (1)$$

$$V_C + V_G + V_W = 0.46\ m^3 \quad (2)$$

$$\frac{W}{C+G} = 0.45 \quad (3)$$

$$\frac{G}{C+G} = i \quad (4)$$

where V_C, V_G, V_W, and V_S [m^3] are the volumes of CEMII, RWGP, water, and sand, respectively. W, C, and G [kg] are the contents (per cubic meter of mortar) of water, CEMII, and RWGP, respectively. i [–] is the cement substitution ratio. To ensure the creation of homogeneous mortar mixtures with minimal bleeding and segregation, as well as good workability, the volume of paste was set to 0.46 m^3 (Equation (2)), and the water-to-binder ratio was chosen as 0.45 (Equation (3)). This water-to-binder ratio was selected to be sufficiently high to alleviate self-desiccation resulting from hydration [38]. A reference mortar mixture, labeled "C", was prepared using CEMII exclusively (i.e., G = 0). Three additional mortar mixtures were designed with 50 wt% substitution of CEMII with RWGP16, RWGP18, and RWGP25 (i = 0.5), and were referred to as "G16", "G18", and "G25", respectively.

Table 3. Compositions of mortar mixtures [kg/m^3].

	C	**G16**	**G18**	**G25**
CEMII	594	282	282	282
RWGP16	0	282	0	0
RWGP18	0	0	282	0
RWGP25	0	0	0	282
Water	267	254	254	254
Sand	1345	1345	1345	1345
Water/Binder [-]	0.45	0.45	0.45	0.45
Clinker in CEMII [kg/m^3]	541	257	257	257
Water/Cement [-]	0.45	0.90	0.90	0.90

Samples were prepared for testing of dry density, Portlandite content, water porosity, flexural and compressive strength (as described in Section 2.3) by casting mortar mixtures into 4 × 4 × 16 cm molds (with six molds per mortar) according to EN 196-1 standard [39]. The molds were stored for 24 h in a room maintained at 26 ± 2 °C and 48 ± 7% RH. After 1 day of casting, the specimens were demolded and subsequently cured under tap water at 26 ± 2 °C prior to testing.

For measuring the water demand and initial setting time (as described in Section 2.3), paste mixtures were prepared with normal consistency using Equations (5)–(7):

$$V_{C^*} + V_{G^*} + V_{W^*} = 1\ m^3 \quad (5)$$

$$\frac{G^*}{C^* + G^*} = i^* \quad (6)$$

$$\frac{W^*}{C^* + G^*} = \omega \quad (7)$$

where V_{C^*}, V_{G^*}, and V_{W^*} [m^3] are the volumes of CEMII, RWGP, and water, respectively. G^*, C^*, and W^* [kg] are the contents (per cubic meter of paste) of RWGP, CEMII, and water, respectively. i^* [–] is the cement substitution ratio. ω [–] is the water-to-binder ratio. A reference paste mixture denoted as "C*" was designed using only CEMII (with G* = 0), while three other paste mixtures were designed by substituting 50 wt% of CEMII with RWGP16, RWGP18, or RWGP25 (i* = 0.5), and were denoted as "G16*", "G18*", and "G25*", respectively. Normal consistency (corresponding to ω) for these mixtures was determined by gradually adding water until the Vicat probe stopped at 6 ± 1 mm from the mold bottom [40]. Table 4 summarizes the proportions used for each of the four paste mixtures to achieve normal consistency.

Table 4. Compositions of paste mixtures with normal consistency [kg/m^3].

	C*	**G16***	**G18***	**G25***
CEMII	1627	729	757	774
RWGP16	0	729	0	0
RWGP18	0	0	757	0
RWGP25	0	0	0	774
Water	472	467	447	434
Clinker in CEMII [kg/m^3]	1481	663	689	704
Water/Cement [-]	0.29	0.64	0.59	0.56

It should be noted that when RWGP is used as a partial substitution for CEMII in both mortar and paste mixtures, the amount of clinker is halved due to the cement dilution effect (CEMII being composed of 91% clinker). Additionally, the water-to-cement ratio (W/C) is doubled.

2.3. Testing Methods

2.3.1. Mini-Conical Slump Test

The workability of the mortar mixtures was characterized using a mini-conical slump test conducted at 26 ± 2 °C and 48 ± 7% RH. The test was performed with a mini-cone featuring a top diameter of 70 mm, a bottom diameter of 80 mm, and a height of 40 mm [41]. To conduct the test, the freshly mixed mortar (Table 3) was introduced into the mini-cone and slowly lifted to allow the mortar to flow under its own weight. Four measurements were performed for each mortar mixture.

2.3.2. Water Demand and Initial Setting Time Determination

Water demand and initial setting time were determined on paste mixtures with normal consistency (Table 4) using a Controls® Vicat apparatus following the EN 196-3 standard [40]. The water demand, which corresponds to the water-to-binder ratio (Equation (7)) necessary to achieve a normal consistency of paste mixture [40], was determined as described in Section 2.2. Three measurements were taken per paste mixture.

The initial setting time, corresponding to the time at which the Vicat needle stops at 4 ± 1 mm from the mold bottom [40], was measured three times per paste mixture.

2.3.3. Fresh and Dry Density Measurement

Fresh density was measured by introducing freshly mixed mortar (Table 3) into a Ø7×14 cm mold and weighing it at 26 ± 2 °C and 48 ± 7% RH. The fresh density ρ_f [g/cm^3] was determined using Equation (8):

$$\rho_f = \frac{m_f}{V_a} \quad (8)$$

where m_f [g] is the mass of the fresh mortar. V_a [cm^3] is the mold apparent volume. Three measurements per mortar mixture were realized.

Dry density was measured at 91 days on 4 × 4 × 4 cm mortar samples (Table 3), which were saw-cut from 4 × 4 × 16 cm specimens (Section 2.2), according to the NF P18-459 standard [42]. This age was chosen because the pozzolanic reaction of RWGP is most significant at later ages [14]. The dry density ρ_d [g/cm^3] was determined by Equation (9):

$$\rho_d = \frac{m_d}{V_s} \quad (9)$$

where m_d [g] is the mass of the dry mortar sample after oven-drying at 55 ± 5 °C. V_s [cm^3] is the volume of the sample measured by hydrostatic weighing. Four measurements per mortar were made.

2.3.4. Semi-Adiabatic Calorimetry

The time-evolution of hydration temperature was monitored by semi-adiabatic calorimetry, which was carried out at 20.5 ± 0.5 °C using a Langavant calibrated calorimeter following the EN 196-9 standard [43]. The procedure involved introducing freshly mixed mortar (Table 3) into the calorimeter to monitor its temperature evolution. Two measurements per mortar mixture were performed.

2.3.5. Thermogravimetric Analysis

The time-evolution of Portlandite content was determined by thermogravimetric analysis using a Setaram Setsys Evolution® device. Measurements were carried out on ~140 mg mortar powders (Table 3) in argon atmosphere, where the powders were subjected to a temperature ramp of 10 °C/min from 25 °C to 1000 °C. The Portlandite contents were determined at 1, 7, 28, and 91 days. The powders tested were obtained from crushing and grinding fragments from 4 × 4 × 16 cm specimens (Section 2.2). The Portlandite content CH [%] was determined by Equation (10):

$$CH = \frac{\Delta m}{m} . \frac{M_{CH}}{M_{H_2O}} .100 \quad (10)$$

where Δm [mg] is the powder mass loss between ~400 and ~600 °C [14]. These two temperatures were adjusted for each powder using the derivative thermogravimetry DTG. m [mg] is the mass of the powder. M_{CH} and M_{H_2O} [kg/mol] are the molecular weights of Portlandite and water, respectively. Two measurements per mortar were taken.

2.3.6. Water Porosimetry

To monitor the time-evolution of porosity, the water saturation under vacuum method was used, following the NF P18-459 standard [42]. The procedure involved placing the samples in a desiccator and maintaining the pressure below 25 mbar for at least 4 ± 0.5 h. The samples were then saturated with water and fully immersed after 15 min, with reduced pressure maintained for 44 ± 1 h. Measurements were taken at 1, 7, 28, and 91 days on

4 × 4 × 4 cm mortar samples (Table 3) obtained by saw-cutting 4 × 4 × 16 cm specimens (Section 2.2). The water porosity Ø [%] was determined by Equation (11):

$$Ø = \frac{m_{sat.} - m_{dry}}{\rho_w V}.100 \quad (11)$$

where $m_{sat.}$ and m_{dry} [kg] are the sample masses measured after water-saturation under vacuum and after oven-drying at 55 ± 5 °C, respectively. ρ_w [kg/m^3] is the water density. V [m^3] is the volume of the sample measured by hydrostatic weighing. Four measurements per mortar were realized.

2.3.7. Flexural and Compressive Strength Test

The time-evolution of both flexural and compressive strength was determined in accordance with the EN 196-1 standard [39]. Measurements were carried out at 1, 7, 28, and 91 days on 4 × 4 × 16 cm mortar specimens (Section 2.2). For each mortar, four measurements were taken for flexural strength, while eight measurements were taken for compressive strength.

3. Results and Discussion

3.1. Slump

Figure 2 shows the slumps measured on the mortar mixtures (Table 3) using a mini-cone. When compared to the reference mortar mixture, the mini-conical slump decreased by 23.1 and 15.4% with partial substitution of CEMII with RWGP16 and RWGP18, respectively. On the other hand, partial substitution with RWGP25 resulted in a 19.2% increase in slump. Despite being less fine than CEMII (Table 2) and having a smooth [13] and hydrophobic [18] surface, RWGP16 and RWGP18 did not increase the slump due to their shape (angular [15], irregular [14], with high aspect ratio [18], and sharp edges [21]) dominating over their granularity and surface condition (smooth and hydrophobic). In contrast, RWGP25 was coarse enough to enhance the fluidity [19] and increase the mini-conical slump. In this case, the coarse granularity and surface condition of RWGP appeared to dominate over its shape.

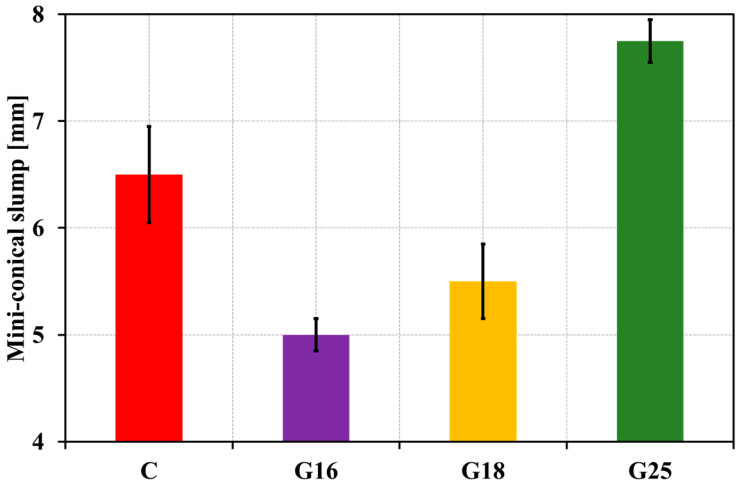

Figure 2. Slumps measured on mortar mixtures using a mini-cone.

A comparison of the three mortar mixtures containing RWGP reveals that the mini-conical slump increases as the granularity of RWGP becomes coarser. This finding is consistent with the results obtained by [28] for cement substitution ratios ≤ 25 wt%. As the granularity of RWGP becomes coarser, its surface condition and coarse granularity compensate for the loss of fluidity caused by its shape. On the other hand, as the granularity of RWGP becomes finer (but still less fine than CEMII), its shape compensates for the gain in fluidity due to its coarse granularity (compared to cement) and surface condition.

It is worth noting that there could be at least one other RWGP between RWGP18 and RWGP25 (between the two granularities) that could allow the mortar mixture to achieve the same fluidity as the reference. In such a case, the effects of the shape, granularity, and surface condition of RWGP would neutralize each other to obtain a similar fluidity as the reference.

3.2. Water Demand

Figure 3 illustrates the water demands required to achieve normal consistencies of paste mixtures (Table 4) based on water-to-binder ratios (Equation (7)) determined by the Vicat apparatus. In comparison to the reference paste mixture, the partial substitution of CEMII with RWGP16 and RWGP18 leads to a 10.3 and 1.7% increase in water demand, respectively. Conversely, the partial substitution of CEMII with RWGP25 results in a 3.4% decrease in water demand. Although RWGP16 and RWGP18 have a less fine granularity than CEMII (Table 2) and are hydrophobic [11], they are not coarse enough to reduce the water demand [20]. It is possible that the shape (angular [15], irregular [14], with high aspect ratio [18], and sharp edges [21]) of RWGP16 and RWGP18 could have contributed to their ability to retain water. This suggests that in this case, the shape of the RWGP particles may be more important than their granularity and surface condition. On the other hand, RWGP25 is coarse enough to decrease the water demand [20], and in this case, it seems that the coarse granularity and surface condition of RWGP may have a greater influence on water retention than its shape.

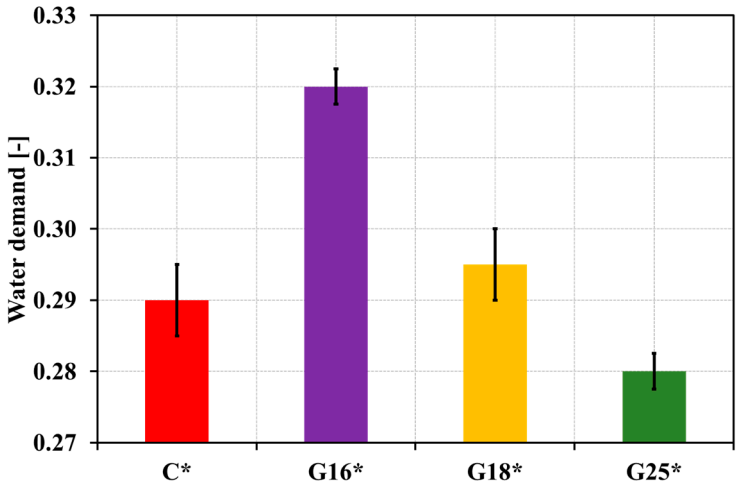

Figure 3. Water demands (water-to-binder ratios) determined on paste mixtures using a Vicat apparatus.

Comparing the three paste mixtures designed with RWGP reveals that the water demand decreases as the granularity of RWGP becomes coarser. This is attributed to the compensatory effect of the surface condition and coarse granularity of RWGP, which are known to decrease water demand [11,18,19,21]. As the granularity of RWGP becomes coarser, the compensatory effect becomes stronger, thereby offsetting the increase in water demand caused by its shape. On the other hand, as the granularity of RWGP becomes finer (but still less fine than CEMII), its shape compensates for the decrease in water demand due to its coarse granularity (compared to cement) and surface condition.

It is worth noting that there might be at least one other RWGP particle size between RWGP18 and RWGP25 that could enable the paste mixture to achieve the same water demand as the reference.

It is also worth noting that the results of water demand (Figure 3) are consistent with those of mini-conical slump (Figure 2). When RWGP is used as partial substitution for CEMII, the water-to-cement ratio of mortar mixtures increases from 0.45 to 0.90 due to the cement dilution effect, as shown in Table 3. It should be emphasized that the hydrophobicity of RWGP leads to more water being available, especially free water. Therefore, the mortar

mixtures with RWGP16 and RWGP18 should have higher fluidity than the reference mixture [11,20,29]. However, since their water demand is higher than that of the reference, they have less free water, which increases the friction between solid particles and reduces their fluidity [13], leading to a decrease in their slump. In this case, the water demand seems to predominate over the effective water-to-cement ratio. On the other hand, the mortar mixture with RWGP25 should have the highest amount of free water due to its low water demand combined with a high effective water-to-cement ratio, resulting in higher fluidity than the reference mixture. It is also evident that the coarser the granularity of RWGP, the lower the water demand, and, thus, the higher the fluidity. This concordance between water demand and slump has been highlighted by [26] for cement substitution ratios $\leq$ 25 wt%.

3.3. Initial Setting Time

Figure 4 displays the initial setting times of paste mixtures with normal consistency (Table 4), which were determined using a Vicat apparatus. The partial substitution of CEMII with RWGP16, RWGP18, and RWGP25 results in an increase of 22.0, 21.3, and 20.5% in the initial setting time, respectively, compared to the reference paste mixture.

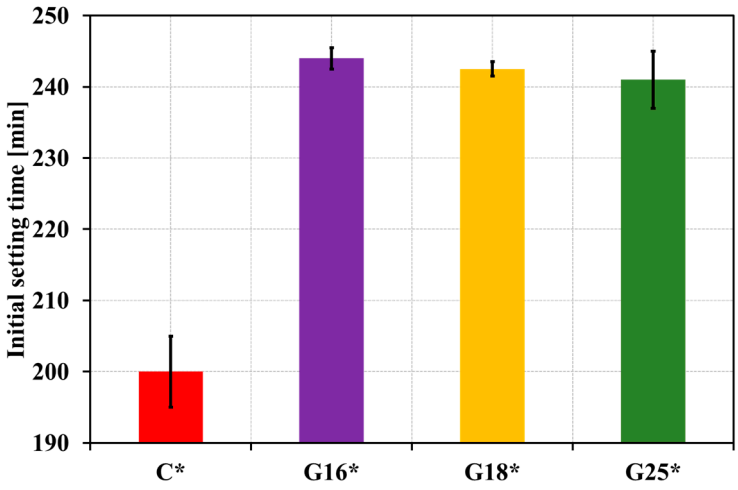

Figure 4. Initial setting times determined on paste mixtures using a Vicat apparatus.

The increase in initial setting time is attributed to two main factors. Firstly, there is a reduction in the overall hydration level (as discussed in Sections 3.5 and 3.6) due to both the cement dilution effect [22], which resulted in halving the amount of clinker (Table 4), and the slow pozzolanic reaction of RWGP at early age [23] (as highlighted in Section 3.6). Secondly, there is an increment in the effective water-to-cement ratio due to the cement dilution effect [14], which doubles the water-to-cement ratio (Table 4), and the hydrophobicity of RWGP [19], which increases the amount of water actually available [12].

It should be noted that the increase in the amount of water available, resulting from both the cement dilution effect and the hydrophobicity of RWGP, is not enough to compensate for the reduction in the overall hydration level. This reduction is due to the significant decrease in the amount of clinker, as well as the slow pozzolanic reaction of RWGP at early age. As a result, the initial setting time increases despite the larger availability of water.

When comparing the three paste mixtures containing RWGP, it can be observed that the initial setting time only slightly decreases as the granularity of RWGP becomes coarser. This trend is not significant, as the change in initial setting time is minimal. One might expect that the decrease in initial setting time would be more pronounced as the granularity of RWGP becomes coarser, due to two factors: (i) the lower water-to-cement ratio (Table 4), and (ii) the higher amount of clinker (Table 4), which leads to a higher level of hydration [44]. However, as observed in the experiments, the decrease in initial setting time is only slightly affected by the coarseness of RWGP. The unexpected behavior of the initial setting time

in relation to the coarseness of RWGP could be explained by the following observations: (i) coarser RWGP leads to lower water demand (Figure 3), resulting in a higher amount of water being available, and (ii) coarser RWGP also provides fewer nucleation sites for the pozzolanic reaction (as discussed in Sections 3.5 and 3.6), which leads to a slower overall hydration level. These factors work in opposite directions and may partially cancel each other out, resulting in only a slight change in initial setting time. The slight changes in initial setting time observed suggest that the range of RWGP granularities studied does not have a significant effect on the initial setting time. This finding is consistent with the conclusion of a previous study [45], which examined a cement substitution ratio of 20 wt% and found a similar lack of significant effect on initial setting time.

3.4. Fresh and Dry Density

Figure 5 provides both the fresh densities of freshly mixed mortars (Table 3) and the dry densities of 4 × 4 × 4 cm mortar samples after 91 days of water curing. Partial substitution of CEMII with different variants of RWGP leads to a decrease of ~4% in fresh density and ~7% in dry density compared to the reference mortar. The lower densities are attributed to the density of RWGP, which is ~20% lower than that of CEMII, as shown in Table 2. This finding is consistent with previous literature with cement substitution ratios $\leq$ 40 wt% [19,24].

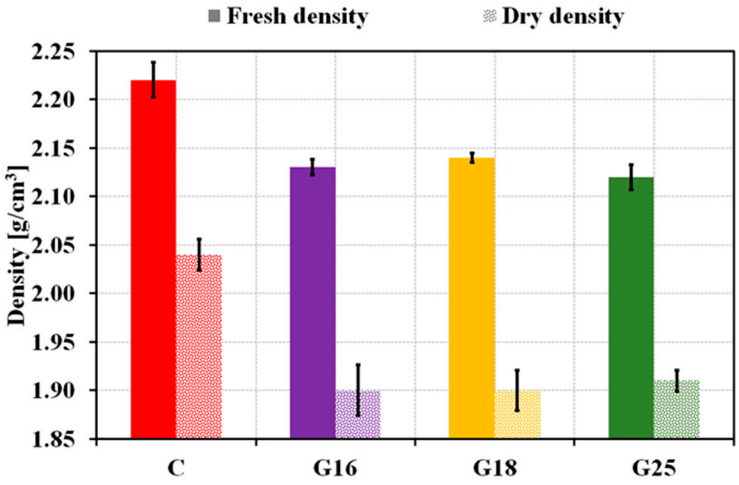

Figure 5. Fresh densities measured on freshly mixed mortars and dry densities determined on 91-day mortar samples.

The three mortars containing RWGP were compared to evaluate the effect of the RWGP granularity on fresh and dry density. There was no significant difference observed in the densities among RWGP16, RWGP18, and RWGP25, as they have the same density (Table 2). Consequently, the resulting mortars had nearly identical densities (fresh or dry).

3.5. Hydration Temperature

Figure 6 presents the time-evolution of hydration temperatures measured on freshly mixed mortars (Table 3) by semi-adiabatic calorimetry. Partial substitution of CEMII with RWGP16, RWGP18, and RWGP25 results in a reduction in the maximum temperature reached during hydration, with decreases of 29.0, 30.2, and 32.3%, respectively, compared to the reference mortar mixture. The decrease in the maximum temperature reached during hydration upon partial substitution of CEMII with RWGP16, RWGP18, and RWGP25 is attributed to the reduction in the overall hydration level (Section 3.6) resulting from both (i) the cement dilution effect [22], which reduces the amount of clinker by half (Table 3), and (ii) the slow pozzolanic reaction of RWGP at early age [12], as highlighted in Section 3.6.

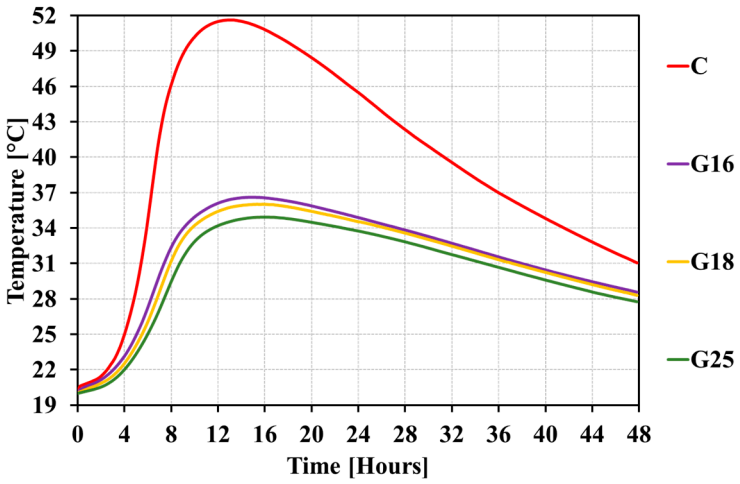

Figure 6. Time-evolution of hydration temperatures measured on freshly mixed mortars by semi-adiabatic calorimetry.

As discussed in Section 3.3, the larger availability of water, resulting from the cement dilution effect and the hydrophobicity of RWGP, is unable to fully compensate for the reduction in overall hydration level caused by the significant decrease in clinker content and the slow pozzolanic reaction of RWGP at early age.

The comparison between the three mortar mixtures containing RWGP reveals a slight downward trend in the maximum temperature reached during hydration as the granularity of RWGP becomes coarser (36.6, 36.0, and 34.9 °C for G16, G18, and G25, respectively). This trend is somewhat unexpected, as coarser RWGP should provide fewer nucleation sites [22,29] and exhibit a slower pozzolanic reaction [29], leading to a lower level of overall hydration (Section 3.6) and a more pronounced reduction in maximum temperature. However, the coarser the granularity of RWGP, the lower the water demand (Figure 3), resulting in a higher amount of water available to compensate for the decrease in hydration temperature. Therefore, although the granularity of RWGP has some effect, the slight variations in maximum temperatures indicate that the range of RWGP granularities studied does not significantly affect the hydration temperature. This finding is consistent with previous studies [18,45] that investigated a cement substitution ratio of 20 wt%.

3.6. Portlandite Content

Figure 7 shows the time-evolution of Portlandite contents measured on mortar powders (Table 3) by thermogravimetric analysis. In the reference mortar, the Portlandite content increases over time as CEMII continuously hydrates [44]. In mortars containing RWGP, the Portlandite content initially increases from 1 to 7 days due to the predominance of CEMII hydration over the slow pozzolanic reaction of RWGP [23,31]. After 7 days, the Portlandite content begins to decrease as the pozzolanic reaction of RWGP accelerates and increasingly predominates over CEMII hydration. Partial substitution of CEMII with different variants of RWGP leads to a reduction in the Portlandite content by approximately 40, 45, 60, and 76% at 1, 7, 28, and 91 days, respectively, compared to the reference mortar. The reduction in Portlandite content observed in the RWGP-containing mortars, compared to the reference mortar, is attributed to two main factors. Firstly, the decrease in the level of hydration (which occurs regardless of time), due to the cement dilution effect [25] that halves the amount of clinker (Table 3), leads to a decrease in Portlandite content. Secondly, the pozzolanic reaction of RWGP gradually converts part of the Portlandite into C-S-H [14] starting from 7 days and beyond. Notably, the level of pozzolanic reaction of RWGP is highest at 91 days, which further contributes to the reduction in Portlandite content.

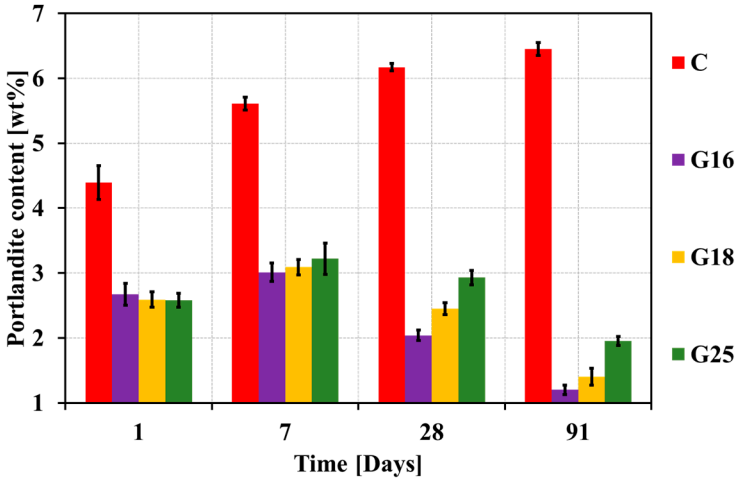

Figure 7. Time-evolution of Portlandite contents measured on mortar powders by thermogravimetric analysis.

After 1 day, a comparison of the three mortars containing RWGP reveals a slight downward trend in Portlandite content as the granularity of RWGP becomes coarser. However, this reduction in Portlandite content is expected to be more pronounced because coarser RWGP provides fewer nucleation sites [22,29], which leads to lower levels of hydration [29]. This behavior is attributed to two factors. Firstly, as shown in Figure 3, the coarser the granularity of RWGP, the lower the water demand, resulting in a higher amount of water being available. Secondly, the pozzolanic reaction of RWGP also slows down as the granularity becomes coarser [29] (this process is already slow at this stage [12,23]). This partly compensates for the decrease in Portlandite content. However, from 7 days and beyond, the Portlandite content increases as the granularity of RWGP becomes coarser. This trend is more pronounced with time because the pozzolanic reaction of RWGP intensifies over time. Additionally, the coarser the granularity of RWGP, the slower its pozzolanic reaction [29], resulting in higher Portlandite contents. Therefore, the range of RWGP granularities studied has an impact on Portlandite content beyond 7 days, as reported by [10] for a cement substitution ratio of 20 wt%.

3.7. Water Porosity

Figure 8 illustrates the time-evolution of water porosities measured on mortar samples (Table 3) by water saturation under vacuum. Over time, the water porosity of the reference mortar decreases as a result of the ongoing hydration reaction of CEMII. This reaction creates hydrates [44] that gradually fill voids in the microstructure [46]. Similarly, in mortars containing RWGP, the water porosity decreases due to the increase in overall hydration level, which is caused by both the hydration of CEMII and the pozzolanic reaction of RWGP. In addition, when compared to the reference mortar, the partial substitution of CEMII with different variants of RWGP results in an increase in water porosity of approximately 8, 9, 10, and 11% at 1, 7, 28, and 91 days, respectively. The increase in water porosity is attributed to two main factors. Firstly, there is a reduction in the overall hydration level due to the dilution effect of the cement [23], which decreases the amount of clinker by half (Table 3), and the weaker pozzolanic reaction of RWGP when compared to the hydration of cement [18]. Secondly, there is an increase in the effective water-to-cement ratio due to the cement dilution effect [21], which doubles the water-to-cement ratio (Table 3), and the hydrophobic nature of RWGP [26], which provides more water that is readily available [12]. Moreover, due to the partial substitution of CEMII with different RWGP variants causing a decrease in density compared to the reference mortar (Figure 5), this could potentially amplify the increase in water porosity.

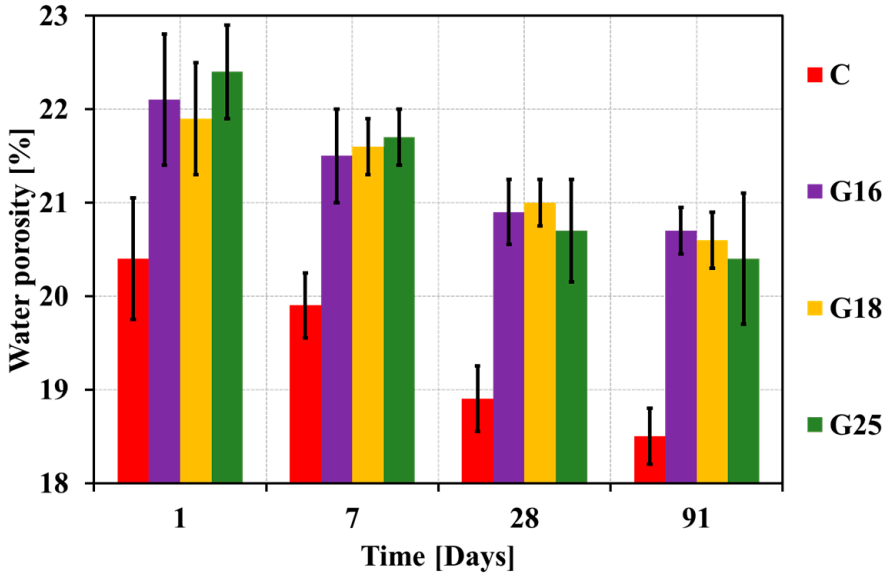

Figure 8. Time-evolution of water porosities measured on mortar samples by water saturation under vacuum.

It is important to note that the weakness of the pozzolanic reaction of RWGP becomes more apparent with time when compared to the hydration of CEMII, since the pozzolanic reaction gradually becomes dominant over the hydration reaction (as discussed in Section 3.6).

The comparison between the three mortars containing RWGP at a given time did not reveal any significant differences in water porosity, making it difficult to draw any definitive conclusions regarding the effect of RWGP granularity on water porosity. However, it is expected that water porosity would increase as the granularity of RWGP becomes coarser, as coarser particles result in a lower overall hydration level and a higher amount of water available (as discussed in Section 3.3, Section 3.5, and Section 3.6). It is possible that the observed lack of difference in water porosity, for a given time, may be due to the relatively low level of distinction that can be achieved by the water saturation under vacuum method (Section 2.3.6), which is commonly used to determine water porosity. This could be due to the hydrophobic nature of RWGP. Further experimental studies are required to confirm these findings.

3.8. Flexural and Compressive Strength

Figure 9 depicts the time-evolution of flexural and compressive strengths measured on mortar specimens (Table 3). The mechanical properties of the reference mortar increase over time due to the ongoing hydration reaction of CEMII, which generates hydrates [44] and densifies the microstructure [46]. Similarly, the mortars containing RWGP exhibit a similar trend, as both CEMII hydration and the pozzolanic reaction of RWGP contribute to the continuous increase in overall hydration level. Furthermore, the mechanical properties of mortars containing different variants of RWGP exhibit a reduction of approximately 50, 40, 25, and 20% compared to the reference mortar at 1, 7, 28, and 91 days, respectively. The reduction in mechanical properties is attributed to two main factors. Firstly, there is a reduction in the overall hydration level resulting from both the cement dilution effect [27], which halves the amount of clinker (Table 3), the weaker pozzolanic reaction of RWGP compared to the hydration of cement [18], and the slower pozzolanic reaction of RWGP at early age [23]. Secondly, there is a rise in the effective water-to-cement ratio due to both the cement dilution effect [21], which doubles the water-to-cement ratio (Table 3), and the hydrophobic nature of RWGP [13], which enhances the availability of water [12]. Furthermore, as the partial substitution of CEMII with different RWGP variants leads to

a decrease in density compared to the reference mortar (Figure 5), this could potentially amplify the decline in mechanical properties.

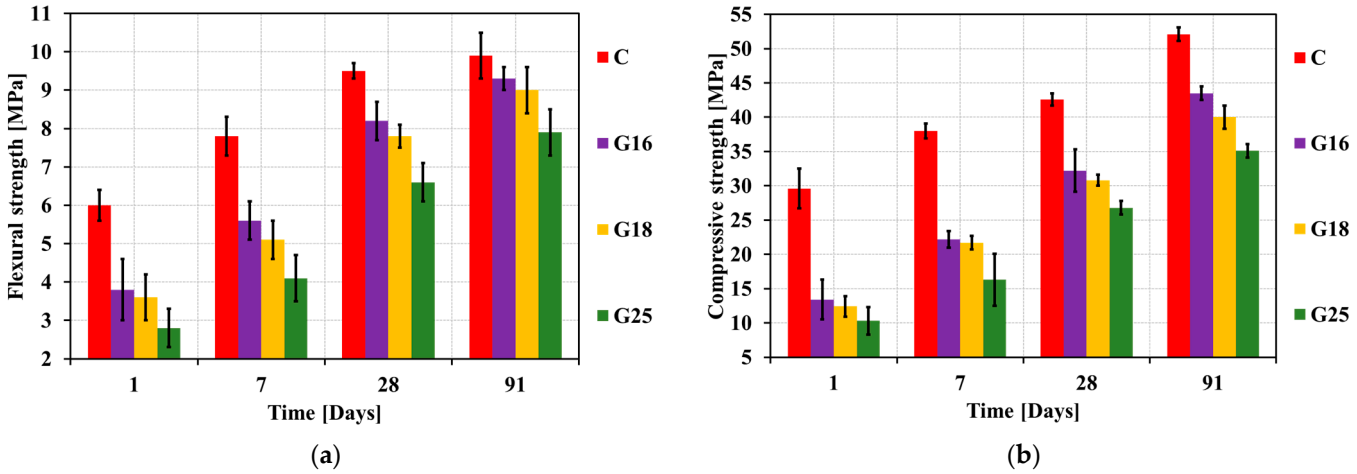

Figure 9. Time-evolution of (**a**) flexural and (**b**) compressive strengths measured on mortar specimens.

The comparison of the three mortars containing RWGP at a given time reveals that the mechanical properties decrease as the granularity of RWGP becomes coarser. This is because coarser RWGP leads to lower overall hydration levels and a higher amount of available water (as discussed in Section 3.3, Section 3.5, and Section 3.6), resulting in a coarser microstructure and lower mechanical properties. Based on these findings, it can be concluded that the range of RWGP granularities studied has a significant impact on mechanical properties. These results align with previous studies on cement substitution ratios $\leq$ 40 wt% [27,30].

4. Conclusions

As glass production continues to increase, the accumulation of glass waste presents significant challenges in terms of storage and disposal. The use of recycled waste glass powder (RWGP) as a partial cement substitute in cement-based materials provides a promising solution to mitigate environmental impact and advance sustainable waste management practices. This study was conducted on a reference material made with Portland-limestone cement CEMII/A-LL42.5R and three other materials containing 50 wt% of recycled waste glass powder (RWGP) with different mean diameters, d_{50}: 16, 18, and 25 µm. The main objective was to analyze the role of RWGP granularity in the short- and medium-term properties of the materials. The results showed that coarser RWGP granularity increased the fluidity and Portlandite content but decreased the water demand and mechanical properties. However, the range of RWGP granularities tested did not significantly affect the initial setting time, fresh and dry density, hydration temperature, and water porosity. The findings suggest that the choice of RWGP granularity should depend on the desired properties of the material. Coarser granularities may be preferred for higher fluidity and Portlandite content, while finer granularities may be favored when looking for better mechanical properties.

To gain further insight into the impact of RWGP granularity on material properties, future research could extend the study to finer granularities than that of cement substituted. This extension could help to identify the optimal RWGP granularity for achieving specific material properties and enhance the understanding of how RWGP granularity affects short- and medium-term properties. Additionally, it could provide valuable information on the impact of RWGP granularity on long-term durability and performance.

Author Contributions: Conceptualization, A.Y., A.E.A.H. and E.B.-A.; methodology, A.Y., A.E.A.H. and E.B.-A.; validation, A.Y., M.A.M., A.E.A.H., R.B. and E.B.-A.; investigation, A.Y. and M.A.M.; resources, A.E.A.H., R.B. and E.B.-A.; data curation, A.Y. and M.A.M.; writing—original draft preparation, A.Y.; writing—review and editing, A.Y., M.A.M., A.E.A.H., R.B. and E.B.-A.; visualization, A.Y., M.A.M., A.E.A.H., R.B. and E.B.-A.; supervision, A.Y., A.E.A.H. and E.B.-A. All authors have read and agreed to the published version of the manuscript.

Funding: This research received no external funding.

Data Availability Statement: The manuscript comprehensively includes all the data that supports the reported results.

Acknowledgments: The authors gratefully thank Pierre-Yves Mahieux (LaSIE UMR CNRS 7356, La Rochelle University) for supplying the Langavant calorimeters.

Conflicts of Interest: The authors declare no conflict of interest.

References

1. Wojtacha-Rychter, K.; Kucharski, P.; Smolinski, A. Conventional and Alternative Sources of Thermal Energy in the Production of Cement—An Impact on CO_2 Emission. *Energies* **2021**, *14*, 1539. [CrossRef]
2. Nie, S.; Zhou, J.; Yang, F.; Lan, M.; Li, J.; Zhang, Z.; Chen, Z.; Xu, M.; Li, H.; Sanjayan, J.G. Analysis of Theoretical Carbon Dioxide Emissions from Cement Production: Methodology and Application. *J. Clean. Prod.* **2022**, *334*, 130270. [CrossRef]
3. Sanjuán, M.Á.; Andrade, C.; Mora, P.; Zaragoza, A. Carbon Dioxide Uptake by Cement-Based Materials: A Spanish Case Study. *Appl. Sci.* **2020**, *10*, 339. [CrossRef]
4. Habert, G.; Miller, S.A.; John, V.M.; Provis, J.L.; Favier, A.; Horvath, A.; Scrivener, K.L. Environmental Impacts and Decarbonization Strategies in the Cement and Concrete Industries. *Nat. Rev. Earth Environ.* **2020**, *1*, 559–573. [CrossRef]
5. Deng, Q.; Zou, S.; Xi, Y.; Singh, A. Development and Characteristic of 3D-Printable Mortar with Waste Glass Powder. *Buildings* **2023**, *13*, 1476. [CrossRef]
6. El-Mandouh, M.A.; Hu, J.-W.; Abd El-Maula, A.S. Behavior of Waste Glass Powder in Concrete Deep Beams with Web Openings. *Buildings* **2022**, *12*, 1334. [CrossRef]
7. Ghareeb, K.S.; Ahmed, H.E.; El-Affandy, T.H.; Deifalla, A.F.; El-Sayed, T.A. The Novelty of Using Glass Powder and Lime Powder for Producing UHPSCC. *Buildings* **2022**, *12*, 684. [CrossRef]
8. Meyer, C. The Greening of the Concrete Industry. *Cem. Concr. Compos.* **2009**, *31*, 601–605. [CrossRef]
9. Gartner, E.; Hirao, H. A Review of Alternative Approaches to the Reduction of CO_2 Emissions Associated with the Manufacture of the Binder Phase in Concrete. *Cem. Concr. Res.* **2015**, *78*, 126–142. [CrossRef]
10. Mirzahosseini, M.; Riding, K.A. Influence of Different Particle Sizes on Reactivity of Finely Ground Glass as Supplementary Cementitious Material (SCM). *Cem. Concr. Compos.* **2015**, *56*, 95–105. [CrossRef]
11. Soliman, N.A.; Tagnit-Hamou, A. Development of Ultra-High-Performance Concrete Using Glass Powder—Towards Ecofriendly Concrete. *Constr. Build. Mater.* **2016**, *125*, 600–612. [CrossRef]
12. Nassar, R.U.D.; Saeed, D.; Al Amara, K.; Room, S. Heat of Hydration, Water Sorption and Microstructural Characteristics of Paste and Mortar Mixtures Produced with Powder Waste Glass; SSRN e-Journal id 4164479. 2022. Available online: https://papers.ssrn.com/sol3/papers.cfm?abstract_id=4164479 (accessed on 10 July 2023).
13. Wang, Y.; Li, Y.; Su, Y.; He, X.; Strnadel, B. Preparation of Waste Glass Powder by Different Grinding Methods and Its Utilization in Cement-Based Materials. *Adv. Powder Technol.* **2022**, *33*, 103690. [CrossRef]
14. Jiang, X.; Xiao, R.; Bai, Y.; Huang, B.; Ma, Y. Influence of Waste Glass Powder as a Supplementary Cementitious Material (SCM) on Physical and Mechanical Properties of Cement Paste under High Temperatures. *J. Clean. Prod.* **2022**, *340*, 130778. [CrossRef]
15. Bouchikhi, A.; Benzerzour, M.; Abriak, N.-E.; Maherzi, W.; Mamindy-Pajany, Y. Study of the Impact of Waste Glasses Types on Pozzolanic Activity of Cementitious Matrix. *Constr. Build. Mater.* **2019**, *197*, 626–640. [CrossRef]
16. Zhang, C.; Wang, J.; Song, W.; Fu, J. Effect of Waste Glass Powder on Pore Structure, Mechanical Properties and Microstructure of Cemented Tailings Backfill. *Constr. Build. Mater.* **2023**, *365*, 130062. [CrossRef]
17. Waldemar, K.; Katarzyna, P.-M.; Krzysztof, S. The Idea of the Recovery of Municipal Solid Waste Incineration (MSWI) Residues in Kłodawa Salt Mine S.A. by Filling the Excavations with Self-Solidifying Mixtures. *Arch. Min. Sci.* **2018**, *63*, 553–565.
18. Lu, J.; Duan, Z.; Poon, C.S. Combined Use of Waste Glass Powder and Cullet in Architectural Mortar. *Cem. Concr. Compos.* **2017**, *82*, 34–44. [CrossRef]
19. Ibrahim, K.I.M. Recycled Waste Glass Powder as a Partial Replacement of Cement in Concrete Containing Silica Fume and Fly Ash. *Case Stud. Constr. Mater.* **2021**, *15*, e00630. [CrossRef]
20. Tognonvi, M.T.; Zidol, A.; Aïtcin, P.-C.; Tagnit-Hamou, A. Aging of Glass Powder Surface. *J. Non-Cryst. Solids* **2015**, *427*, 175–183. [CrossRef]
21. Nahi, S.; Leklou, N.; Khelidj, A.; Oudjit, M.N.; Zenati, A. Properties of Cement Pastes and Mortars Containing Recycled Green Glass Powder. *Constr. Build. Mater.* **2020**, *262*, 120875. [CrossRef]

22. Bazhuni, M.F.; Kamali, M.; Ghahremaninezhad, A. An Investigation into the Properties of Ternary and Binary Cement Pastes Containing Glass Powder. *Front. Struct. Civ. Eng.* **2019**, *13*, 741–750. [CrossRef]
23. Du, H.; Tan, K.H. Properties of High Volume Glass Powder Concrete. *Cem. Concr. Compos.* **2017**, *75*, 22–29. [CrossRef]
24. Rodier, L.; da Costa Correia, V.; Savastano Junior, H. Elaboration of Eco-Efficient Vegetable Fibers Reinforced Cement-Based Composites Using Glass Powder Residue. *Cem. Concr. Compos.* **2020**, *110*, 103599. [CrossRef]
25. Du, Y.; Yang, W.; Ge, Y.; Wang, S.; Liu, P. Thermal Conductivity of Cement Paste Containing Waste Glass Powder, Metakaolin and Limestone Filler as Supplementary Cementitious Material. *J. Clean. Prod.* **2021**, *287*, 125018. [CrossRef]
26. Aliabdo, A.A.; Abd Elmoaty, A.E.M.; Aboshama, A.Y. Utilization of Waste Glass Powder in the Production of Cement and Concrete. *Constr. Build. Mater.* **2016**, *124*, 866–877. [CrossRef]
27. Idir, R.; Cyr, M.; Tagnit-Hamou, A. Pozzolanic Properties of Fine and Coarse Color-Mixed Glass Cullet. *Cem. Concr. Compos.* **2011**, *33*, 19–29. [CrossRef]
28. Li, Q.; Qiao, H.; Li, A.; Li, G. Performance of Waste Glass Powder as a Pozzolanic Material in Blended Cement Mortar. *Constr. Build. Mater.* **2022**, *324*, 126531. [CrossRef]
29. Kamali, M.; Ghahremaninezhad, A. An Investigation into the Hydration and Microstructure of Cement Pastes Modified with Glass Powders. *Constr. Build. Mater.* **2016**, *112*, 915–924. [CrossRef]
30. Shao, Y.; Lefort, T.; Moras, S.; Rodriguez, D. Studies on Concrete Containing Ground Waste Glass. *Cem. Concr. Res.* **2000**, *30*, 91–100. [CrossRef]
31. Liu, G.; Florea, M.V.A.; Brouwers, H.J.H. Performance Evaluation of Sustainable High Strength Mortars Incorporating High Volume Waste Glass as Binder. *Constr. Build. Mater.* **2019**, *202*, 574–588. [CrossRef]
32. *EN 197-1 Standard*; Cement—Part 1: Composition, Specifications and Conformity Criteria for Common Cements. AFNOR: Paris, France, 2011.
33. *ISO 12154 Standard*; Determination of Density by Volumetric Displacement—Skeleton Density by Gas Pycnometry. AFNOR: Paris, France, 2014.
34. *EN 196-6 Standard*; Methods of Testing Cement—Part 6: Determination of Fineness. AFNOR: Paris, France, 2018.
35. *ISO 13320 Standard*; Particle Size Analysis—Laser Diffraction Methods. AFNOR: Paris, France, 2020.
36. Khmiri, A.; Chaabouni, M.; Samet, B. Chemical Behaviour of Ground Waste Glass When Used as Partial Cement Replacement in Mortars. *Constr. Build. Mater.* **2013**, *44*, 74–80. [CrossRef]
37. *EN 13139 Standard*; Aggregates for Mortar. AFNOR: Paris, France, 2003.
38. Jensen, O.M. Thermodynamic Limitation of Self-Desiccation. *Cem. Concr. Res.* **1995**, *25*, 157–164. [CrossRef]
39. *EN 196-1 Standard*; Methods of Testing Cement—Part 1: Determination of Strength. AFNOR: Paris, France, 2016.
40. *EN 196-3 Standard*; Methods of Testing Cement—Part 3: Determination of Setting Times and Soundness. AFNOR: Paris, France, 2016.
41. Bouvet, A.; Ghorbel, E.; Bennacer, R. The Mini-Conical Slump Flow Test: Analysis and Numerical Study. *Cem. Concr. Res.* **2010**, *40*, 1517–1523. [CrossRef]
42. *NF P18-459 Standard*; Concrete—Testing Hardened Concrete—Testing Porosity and Density. AFNOR: Paris, France, 2022.
43. *EN 196-9 Standard*; Methods of Testing Cement—Part 9: Heat of Hydration—Semi-Adiabatic Method. AFNOR: Paris, France, 2010.
44. Midgley, H.G. The Determination of Calcium Hydroxide in Set Portland Cements. *Cem. Concr. Res.* **1979**, *9*, 77–82. [CrossRef]
45. Lu, J.; Duan, Z.; Poon, C.S. Fresh Properties of Cement Pastes or Mortars Incorporating Waste Glass Powder and Cullet. *Constr. Build. Mater.* **2017**, *131*, 793–799. [CrossRef]
46. Rougelot, T.; Skoczylas, F.; Burlion, N. Water Desorption and Shrinkage in Mortars and Cement Pastes: Experimental Study and Poromechanical Model. *Cem. Concr. Res.* **2009**, *39*, 36–44. [CrossRef]